6-1993

The Development and Testing of an Instrument for Doing Fast Time-Resolved Infrared Spectroscopy and the Study of Dimanganese Decacarbonyl Using UV/VIS and FTRIR Spectroscopic Techniques

Steven Wells Kinne
Union College - Schenectady, NY

THE DEVELOPMENT AND TESTING OF AN INSTRUMENT FOR DOING FAST TIME-RESOLVED INFRARED SPECTROSCOPY AND THE STUDY OF DIMANGANESE DECACARBONYL USING UV/VIS AND FTRIR SPECTROSCOPIC TECHNIQUES

By

Steven Wells Kinne

****

Submitted in partial fulfillment
of the requirements for
Honors in the Department of Chemistry

UNION COLLEGE

June, 1993

Abstract

KINNE, STEVEN WELLS The Development and Testing of an Instrument for Doing Fast Time-Resolved Infrared Spectroscopy and the Study of Dimanganese Decacarbonyl Using UV/VIS and FTRIR Spectroscopic Techniques. Department of Chemistry, June 1993.

Over the past three years at Union College, an instrument has been developed that can be used to probe the mechanisms of the photochemistry of transition metal carbonyl compounds. When these complexes are activated with photons, one or two carbonyl ligands are removed from the complex, opening these sites for chemical bonding. Thus, the coordinatively unsaturated species become catalytically active, and can catalyze a wide variety of organic reactions. The intermediates in these catalytic cycles tend to be short-lived (lifetimes are usually less than one second), and therefore special instrumnetation must be developed in order to directly observe these intermediates spectrally.

The instrument that has been built can be used to perform flash photochemical studies of these catalysts and the catalyzed organic reactions. The photolysis light sources are xenon flashlamps, and the probe light is a tunable diode IR laser operating in the range of 1700-2100 cm^{-1} (the CO stretching region). Signals are collected on a digital oscilloscope for transfer to a computer, where kinetic analyses are performed.

The instrument was tested by studying the kinetics of dimanganese decacarbonyl, a transition metal carbonyl whose kinetics have been well-characterized in the literature. This kinetic study was performed on both the recently completed FTRIR flash rig and the already existing UV/VIS flash rig for two purposes. The first was to test the new instrument and the procedures involved in this experiment. The second was to develop new kinetic experiments for the Physical Chemistry laboratory at Union College.

Acknowledgements

The author would like to thank the National Science Foundation for their contribution to the completion of the FTRIR flash rig in the form of an Instruments for Laboratory Improvement grant. Thanks should also be given to the Dow Chemical Company and Union College for providing stipends for summer research.

Thanks for technical support goes to the Union College Machine Shop and the Electronics Shop in the Electrical Engineering Department at Union College, for the important assistance provided.

Finally, the author would especially like to thank Prof. David M. Hayes, whose consummate knowledge, sage advice and countless witticisms have made this research a successful and mind-broadening experience.

Steven W. Kinne

Eye to I,
Reaction burning hotter,
Two to one,
Reflection on the water...

H to O,
No flow without the other,
Oh but how
Do they make contact with one another?

Electricity? Biology?
Seems to me it's Chemistry...

- Rush, "Chemistry"

Table of Contents

Table of Figures

Chapter 1: Background

Introduction

During the past three decades, scientists have had a great interest in studying transition metal carbonyls because of the catalytic properties of this class of compounds. Transition metal carbonyls are known to catalyze a wide variety of organic reactions, including insertion reactions, olefin isomerization reactions, and the hydrogenation and hydrosilation of unsaturated hydrocarbons. These compounds act as catalyst precursors, in that an excitation of some sort is required to initiate catalysis. This excitation typically involves the dissociation of one or two ligands from the transition metal center. Early studies involved thermal excitation processes, but more recent experimentation has concentrated on the photoactivation of these precursors. Because transition metal carbonyls can be activated through photolysis, the energy efficiency and selectivity of the catalysis reactions can be greatly increased. These activated carbonyls act as true photocatalysts, in that the formation of the photocatalytic species from the precursor requires only the initial absorbance of one or two photons. These catalysis reactions can proceed in the dark after the initial photoactivation, and thus quantum yields for these reactions typically exceed one.

However, the study of the mechanisms of these catalytic cycles has been hampered for various reasons. Transition metal carbonyls tend to be both air- and water-sensitive, thus making them challenging to work with in the laboratory. Precautions must be taken to ensure the purity of the catalyst precursors so that undesirable side reactions don't appear. Also, many mechanisms have had to be based on indirect methods of proving the existence of reaction intermediates. Due to the short lifetimes (typically <1sec) of these intermediates, direct spectral observation has been rare. Finally, much of the direct spectral observation of reaction intermediates has been performed using UV/VIS absorption spectroscopy which, although being an adequate technique, cannot

compare with the resolution or structural sensitivity of its IR counterpart. The technology for performing fast time-resolved IR spectroscopy has only become available within the last ten years.

The goals of this research project, then, were three-fold. First, an instrument capable of performing fast time-resolved infrared (FTRIR) spectroscopy on a transition metal carbonyl catalyzed reaction cycle in the solution phase (using flash photolysis as an excitation method) was to be developed and debugged. Second, a complete kinetic study of a transition metal carbonyl test system, in this case dimanganese decacarbonyl dissolved in cyclohexane, was to be performed on the already built fast time-resolved UV/VIS flash rig. This was important for two reasons. Because the numerous studies carried out on dimanganese decacarbonyl by other research groups, this system allowed for the testing of solution preparation and purification techniques as well as a method for data analysis. It also presented a feasible experimental method that could be implemented as a laboratory experiment for our Physical Chemistry course at Union. Finally, a similar kinetic study on dimanganese decacarbonyl (dissolved in heptane) was to be performed on the newly built FTRIR flash rig to test the reliability of experimental results from the new instrument. Then, knowing that the instrument is reliable, the kinetics of various steps in proposed catalytic cycles could be determined, and previously unseen reaction intermediates could be directly observed.

$Mn_2(CO)_{10}$ as a Test System

Dimanganese decacarbonyl was chosen as a test system for the flash rigs mentioned above for various reasons. First (and most obviously), it belongs to the class of compounds targeted for study, the transition metal carbonyls. Its properties are similar to those of other transition metal carbonyls, thus providing a good model for the photochemistry that will be encountered in subsequent experiments. Second, its photochemistry has been well-characterized in the literature (1-9). Many studies have

been performed on this compound, and consequently there exists a reliable frame of reference to compare the experimental results gathered in this study. The other advantages of this particular transition metal carbonyl become apparent with an in-depth look at the existing literature.

Three of the aforementioned papers are of great importance because of the similarities to the experimental procedure utilized in this study. In 1977, a communication from Thomas Meyer's research group at the University of North Carolina at Chapel Hill discussed the photochemistry of dimanganese decacarbonyl in cyclohexane and THF solvents (1). They proposed that the main photochemical process happening in this system is the absorption of a photon by $Mn_2(CO)_{10}$ resulting in the breaking of the Mn-Mn bond as seen in Equation 1.

$$Mn_2(CO)_{10} \xrightarrow{h\nu} 2\ Mn(CO)_5 \qquad (1)$$

These two manganese pentacarbonyl fragments subsequently recombine to form the parent compound with some rate constant k.

$$2\ Mn(CO)_5 \xrightarrow{k} Mn_2(CO)_{10} \qquad (2)$$

They monitored the reappearance of $Mn_2(CO)_{10}$ vs. time using UV/VIS absorption techniques and made rate constant calculations from this data.

In 1983, a laser photolysis study of dimanganese decacarbonyl was published by Yesaka's group at the University of Tokyo (2). Again, they studied the photolysis of $Mn_2(CO)_{10}$ in cyclohexane, but observed two separate photoactivation processes. One of the reactions was the breaking of the Mn-Mn bond observed by Meyer's group. The other involved the breaking of an Mn-C bond, resulting in the loss of a CO ligand.

$$Mn_2(CO)_{10} \xrightarrow{h\nu} Mn_2(CO)_9 + CO \qquad (3)$$

Again, the intermediate would reform the parent compound with some rate constant k if no other reactive species were present in solution to compete for $Mn_2(CO)_9$.

$$Mn_2(CO)_9 + CO \xrightarrow{k} Mn_2(CO)_{10} \qquad (4)$$

UV/VIS absorption spectroscopy was used to monitor the disappearances of the two intermediates, which absorbed at two distinct wavelengths (500 nm for $Mn_2(CO)_9$ and 827 nm for $Mn(CO)_5$).

Grevel's group at the Max Planck Institute in Germany published a communication in 1984 which described a study of the kinetics of dimanganese decacarbonyl photochemistry (3) in both cyclohexane and heptane. They observed both of the reaction intermediates that Yesaka mentioned in his paper, and they included a complete list of absorbance peaks for the intermediates in both solvents. The main point of interest regarding this study was the use of both UV/VIS and IR spectroscopy to study these reaction kinetics.

It can be seen from these publications that dimanganese decacarbonyl makes a useful test system for the reasons described above. Furthermore, the photochemistry of this transition metal carbonyl is relatively simple, especially if studied in the absence of other reactive species, consisting only of the formation of the two aforementioned intermediates which subsequently react to reform the parent compound (Eqs. 1-4). Because of this reversibility, this compound is also fairly simple to work with experimentally, as one $Mn_2(CO)_{10}$ solution can be used a number of times. Each reaction intermediate absorbs at a distinct wavelength in both the UV/VIS and IR spectrum, thus allowing each of the recombination reactions to be observed independently. Finally, because this system can be made to react according to both second and pseudo-first order kinetics, it makes an attractive experiment for an undergraduate physical chemistry laboratory.

$Mn_2(CO)_{10}$ Kinetics

In the study of dimanganese decacarbonyl, the kinetics of the two recombination reactions are of interest.

$$Mn_2(CO)_9 + CO \xrightarrow{k_1} Mn_2(CO)_{10} \quad (5)$$

$$2\,Mn(CO)_5 \xrightarrow{k_2} Mn_2(CO)_{10} \quad (6)$$

In both of these cases, the reactions are second order. The differential rate equations for each of these reactions are found below.

$$-d[Mn_2(CO)_9]/dt = k_1[Mn_2(CO)_9][CO] \quad (7)$$
$$-1/2(d[Mn(CO)_5]/dt) = k_2[Mn(CO)_5]^2 \quad (8)$$

When these equations are integrated, they become:

$$1/[Mn_2(CO)_9] = k_1 \cdot t + 1/[Mn_2(CO)_9]_o \quad (9)$$
$$1/[Mn(CO)_5] = 2\,k_2 \cdot t + 1/[Mn(CO)_5]_o \quad (10)$$

Equation 9 may not seem intuitive because it is integrated from a mixed second order rate equation. However, the reaction expressed in Equation 7 is an equal-concentration mixed second order reaction, meaning that the concentraions of $Mn_2(CO)_9$ and CO remain equal throughout the reaction. Thus, it can be treated as if it were of the form below.

$$-d[Mn_2(CO)_9]/dt = k_1[Mn_2(CO)_9]^2 \quad (11)$$

Equation 9 is correct if integrated from Equation 11.

It can be seen that these integrated rate equations are expressed in terms of concentration. For spectroscopic experiments, the absorbance of the material is measured at a particular wavelength. This absorbance can be related to the concentration by Beers' Law, shown below:

$$A = \varepsilon\, l\, c \quad (12)$$

where A is absorbance, ε is the extinction coefficient for the compound at the monitoring wavelength, l is the path length of the optical cell and c is the molar concentration. By applying this relationship to the integrated rate laws, we get the rate equations below.

$$1/A = [k_1/(\varepsilon \cdot l)] \cdot t + 1/A_o \quad (13)$$

$$1/A = [2\ k_2/(\varepsilon \cdot l)] \cdot t + 1/A_o \quad (14)$$

Thus, plots of 1/A vs. time should be linear for each recombination reaction, and the rate constants can be calculated from the slope if ε is known for the absorbing species. But, in many cases, the exact value of ε is not known for the short-lived reaction intermediates being monitored. Two techniques could be used to get around this difficulty. The first would be to estimate a value for ε, as is done in Yesaka's study (2). The second (and more sophisticated) method would be to induce pseudo-first order behavior in the reactions. This method cannot be used with the manganese pentacarbonyl recombination, but can be used easily with the dimanganese nonacarbonyl recombination. By flooding the solution with an excess of CO, it is possible to make the concentration of CO so large that it does not change significantly during the reaction. In this case, the rate equation would become:

$$-d[Mn_2(CO)_9]/dt = k_{obs}[Mn_2(CO)_9] \quad (15)$$

where $k_{obs} = k_1[CO]$. The integrated form of this pseudo-first order rate law, taking into account the Beers' Law relationship (Eq. 12), appears below.

$$\ln A = -k_{obs} \cdot t + \ln A_o \quad (16)$$

By inducing pseudo-first order kinetics using various concentrations of CO, a plot can be made of k_{obs} vs. [CO]. The slope of this plot would be the second order rate constant k_1. Thus, it becomes unnecessary to estimate a value of ε and, in fact, ε can subsequently be calculated from the slope of a plot described by Equation 13 using the value of k_1.

Chapter 2: The Design and Construction of the FTRIR Spectrometer

Instrumental Requirements

The intent of this aspect of the research was to construct a new instrument capable of performing FTRIR absorption spectroscopy on the short-lived reaction intermediates of these photocatalyzed organic reactions. There were various concerns taken into account during the design of this apparatus. Much of the theory was discussed in detail by Gene Bernard (10). A quick overview of the instrumental needs will be provided here.

Since transition metal carbonyls serve only as catalyst precursors, flash photolysis was used as the method of activation to create the actual catalyst. Activation involves dissociation of one or two ligands from the precursor to create a coordinatively unsaturated species which becomes part of the catalytic cycle. The photolysis source had to be a high-intensity light source which produced a wavelength of light capable of energizing the precursor to its catalytic state. The duration of this flash had to be short, because we did not want the light from the lamps interfering with absorbance measurements for the short-lived reaction intermediates. The probe light detector had to have a fast response time for the same reason, as it was necessary to be able to see changes in the absorbances of these short-lived intermediates. The probe light itself had to be of sufficient intensity to provide a sufficiently high signal/noise ratio, and also the probe light's intensity had to remain stable throughout the reaction to provide a reliable baseline. Because of the air- and water-sensitivity of the transition metal carbonyls, special techniques had to be developed for the synthesis and handling of these reaction solutions. We also wished to incorporate a computer into our data analysis system, as this would increase the efficiency of these kinetic analyses.

A schematic diagram of this instrument can be found in Figure 1. Detailed descriptions of each subassembly of this apparatus are provided below.

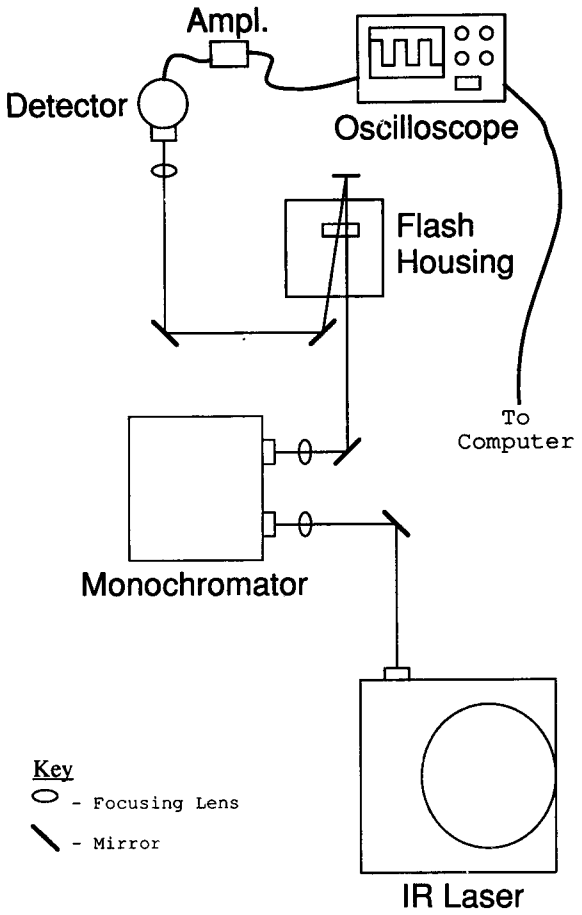

Figure 1: Schematic of the FTRIR flash rig

The Photolysis Source and Flash Housing

For this instrument, the excitation light used in flash photolysis is provided by two xenon flashlamps connected in series by a copper conductor. The lamps are mounted above and below the sample cell within the flash housing. These lamps are powered by a micropulser with an external triggering unit, and are capable of outputting about 400 J/flash. This power corresponds to a high photon flux emitted from the lamps, and thus a high amount of catalyst precursor is activated. The light emitted by the lamps is polychromatic, however, with ultraviolet, visible and infrared photons included. This raises concerns about interference of flashlamp light interfering with absorption measurements in the IR.

The flash housing is designed to minimize any intermingling of scattered light from the flashlamps with the infrared detector. Each lamp is contained within its own compartment, with light being let out through a slot in the container. Filter solution containers can be inserted in front of these slots, thus allowing only certain wavelengths of the flashlamp light to pass out of the compartment and interact with the rest of the instrument (especially the sample cell). Thus, stray IR emissions from the lamps can be filtered out and kept from interfering with absorption measurements. The housing is also designed with the intent of protecting the reaction solution from radiation emanating from within the lab itself, such as photons from the ceiling lamps.

The micropulser that powers the flashlamps discharges at voltages in the range of 8 to 10 kV, and thus transient electronic interference from electromagnetic pulses generated by this high-voltage system becomes a great concern. Through-space electromagnetic pulses could easily interact with the electronics in the detection/data capture system, interfering with our ability to collect reliable kinetic data. To suppress this effect, the high-voltage devices were all enclosed in Faraday cages, constructed from wood frames covered with layers of either copper mesh or copper sheeting. The cages could accomadate small holes in the copper, so that there was no problem with enclosing

the entire flash housing in an independently removable Faraday cage. A hole on either side of the flash housing Faraday cage was cut in order to let the probe light pass through the sample cell.

The advantages of this set-up are readily apparent. The flashlamps are of high intensity, which excites a high concentration of catalyst precursor to the photocatalyst. Any transient radiation from the lamps themselves which could interfere with IR absorption measurements was eliminated by the filter solution system discussed above. Faraday cages serve to isolate the high-voltage components of the system from the detection and data analysis systems, preserving the integrity of the kinetic data. The triggering mechanism for the system allows us to coordinate the initiation of data capture with the discharge of the flashlamps (i.e. the start of the reaction). Finally, the housing itself keeps the relative positions of the lamps and the sample cell constant, a rather obvious advantage.

The Infrared Probe Light

For reasons discussed in detail by Gene Bernard (10), it was determined that the best IR probe source was a tunable diode IR laser operating in the range of 1700 - 2100 cm^{-1}. Briefly, this laser is a very stable and safe source of infrared light. It can be operated on normal line voltage, and through the manipulation of two variables (mentioned later), it is easy to tune through a range of frequencies. However, there are also disadvantages associated with this probe source. The power output of the diode laser is low compared to a CO laser, and also solid state lasers have a property different from most other lasers in that the light produced is somewhat polychromatic. As an example, a sample spectrum of one diode setting is presented in Figure 2. There are several distinct "modes" associated with each setting of the diode.

A monochromator is used with the diode laser to select out the one "mode" that is desired for the absorption measurement. However, the dial on the monochromator being

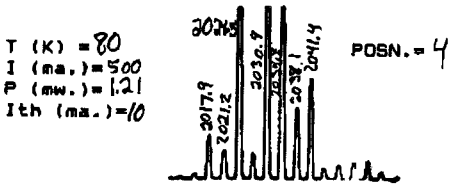

Figure 2: An example spectra from the tunable diode infrared laser

used is numbered arbitrarily. In order to use it as a filter, a method had to be developed to convert between IR frequency and monochromator dial setting. There should be a linear relationship between the dial setting and the wavelength of the incoming IR light. By using a monochromatic light source with a known wavelength (in this case, a HeNe laser), this relationship could be found using the property of diffraction. The grating equation shown below shows that a monochromatic light source diffracted off of a grating produces a series of images. Each image (of a different order) corresponds to a discrete multiple of the laser's wavelength.

$$n\lambda = d(\sin\theta) \tag{17}$$

In the above equation, n is the order of the image, λ is the wavelength of the monochromatic light, d is the spacing between the slits on the grating and θ is the angle at which the beam is diffracted off the grating (measured from the normal of the grating). This relationship can be manipulated to show that the n-th order image of the HeNe laser diffracts at the same angle as the first order image of a light having a wavelength n times larger than the HeNe laser wavelength.

$$n\lambda = d(\sin\theta) = (1)(n\lambda) \tag{18}$$

By using the various order images of the HeNe laser beam, a plot of λ vs. dial setting can be made which gives the relationship between wavelength (and therefore frequency) and the arbitrary monochromator setting. This plot and the best-fit linear equation can be found in Figure 3.

Two variables are used in the tuning of the diode: the current passing through the diode, and the temperature of the diode. Both could be monitored and varied easily using the control equipment supplied with the diode laser. But one was not told which combinations produced which frequencies. Thus, the IR laser was run through the entire range of its current and temperature settings. By using the monochromator and the previously derived calibration equation (Figure 3), the frequency associated with each

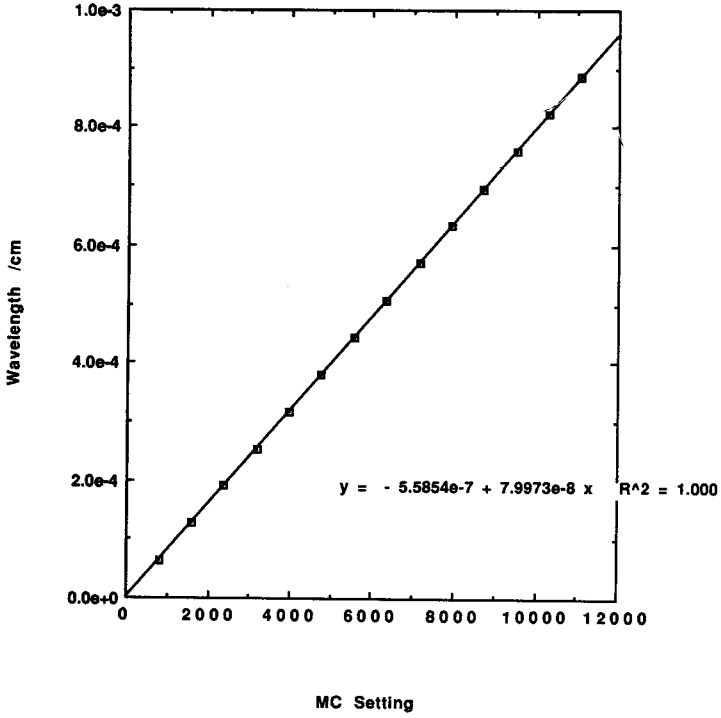

Figure 3: Calibration graph for the monochromator

setting could be determined. A rough plot of frequency vs. current at various temperature settings is found in Figure 4. Each commercially available diode, when taken from 0-0.5A (max I) and from 83-110K (max T), spans a frequency range of approximately 200 cm^{-1}. The diode used in this instrument runs from 1900-2100 cm^{-1}, which is sufficient for the absorbances of interest (the carbonyl stretching frequencies), with the exception of the bridging carbonyl stretching frequencies (between 1750 and 1850 cm^{-1}), which could be seen if another diode is purchsed that spans the range from 1700-1900 cm^{-1}. But for the chemical systems of interest to this research group, the 1900-2100 cm^{-1} range is of greatest importance.

The alignment of the probe beam was also an important step in the construction of the instrument. The light had to be passed through the monochromator, double-passed through the flash housing (and sample cell) and then made to strike the center of the indium antinomide IR detector. A HeNe laser, provided with the diode laser, was used in this alignment process due to the invisibility of the IR beam. By establishing a basis for colinearity between the two beams, the HeNe beam could be used to align the IR beam. A beam splitter within the laser housing was integral in this optical manipulation, by insuring that the beam was parallel to the optical bench and in sending a HeNe beam back to be positioned by an off-axis paraboloid mirror onto the lasing diode. When the HeNe beam struck the diode, one point was established where the HeNe and IR beams were located in the same position. A second point would be established when both beams struck the center of the detector, insuring colinearity. This alignment process was hampered by two problems, though: the invisibility of the IR beam and the lack of completely independent positioning controls for the HeNe and IR beams.

Compromises had to be made in order to maximize both diode output power and resolution. The slits on the monochromator were made extremely narrow (on the order of 0.1 mm) so as to separate IR peaks with a resolution of < 3 cm^{-1}. Filtering out the

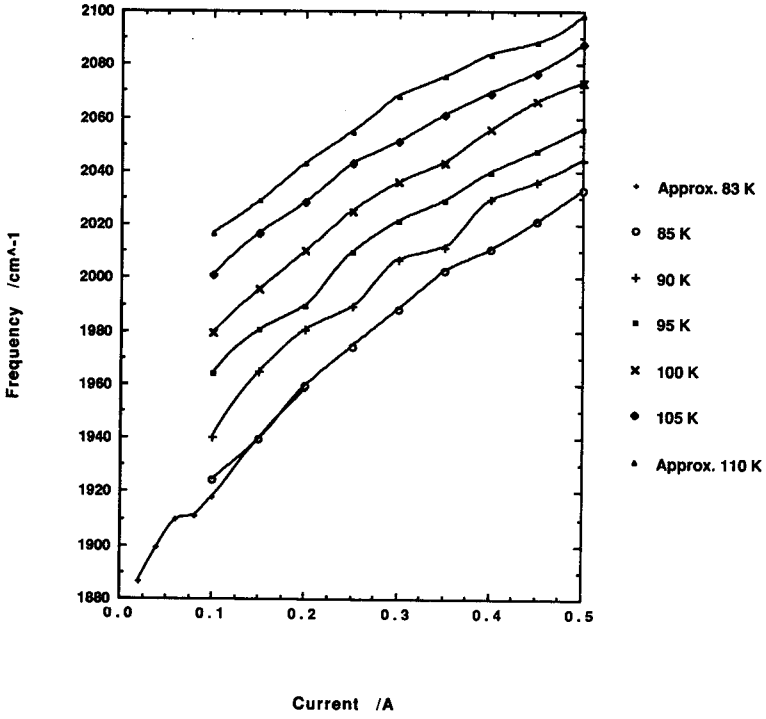

Figure 4: Frequency of diode output shown as a function of temperature and current

unwanted modes lessened the power of the IR beam considerably, but nonetheless allowed enough intensity through for a good signal/noise ratio.

The Sample Cell and the Flow System

The sample cell is a cylinder of stainless steel through which the solutions we are studying can flow. Its thickness has been minimized so that all parts of the solution will be irradiated with the same intensity by the flashlamps (as shadows from overhanging edges could create concentration gradients within the solution and introduce artifacts into the absorbance measurements). The solution passes between two calcium flouride optical plates held in place by a sandwich of O-rings. Specifically, a compressible viton gasket is inserted before the CaF_2 plate to act as a spacer, while a screwable brass O-ring is used to hold the CaF_2 in place (with a teflon O-ring between the brass and the CaF_2 plate to prevent scratching). Inlet and outlet ports on each side of the cell allow the solution to flow between the CaF_2 plates. The path length of this optical cell was minimized because we wanted to minimize the absorbance of the IR probe beam by the solvent. The path length was estimated to be about 1.25 mm. This estimation was made by using the ratios of cyclohexane absorbance peaks measured in a cell of known path length and our sample cell using a FTIR spectrometer.

Although this problem did not exist in the dimanganese decacarbonyl photochemical system, there was concern regarding build-up of reaction products within the sample cell and these compounds interfering with subsequent runs. We did want to have the capability of performing a series of runs without having to prepare new reaction solution for each run. A flow system was incorporated into this instrument for this reason, allowing us to be able to flash a certain volume of the reaction solution, monitor absorbances and then flow in fresh solution for another run. A schematic of this flow system can be found in Figure 5.

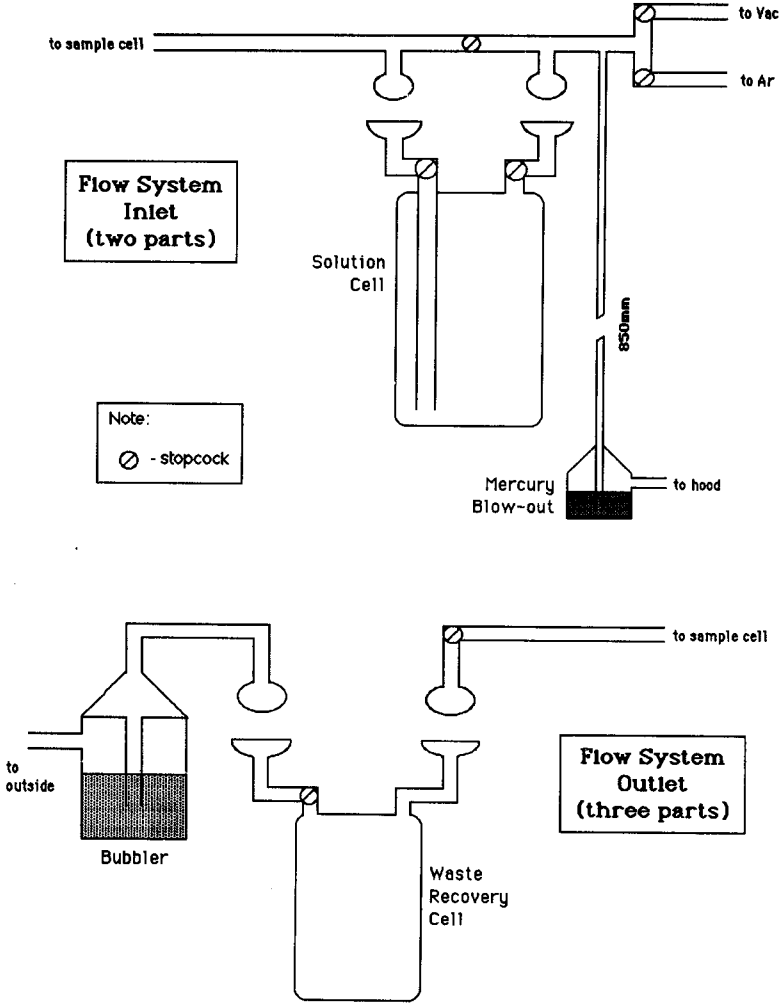

Figure 5: Schematic of the flow system for the FTRIR flash rig

The flow system consists of three main parts: a main direct line attached to a vacuum pump and a tank of pure argon, a reaction solution vessel designed for air-tight transport of solutions to and from the nearby high-vacuum line, and a waste recovery vessel designed to capture used solutions for solvent recovery and safe disposal of potentially hazardous chemicals. The other parts of the system that should be noted are the mercury blow-out, which protects against extreme over-pressures of argon gas in the flow system, and the oil bubbler, which allows for the escape of argon without admitting air into the system.

The flow system can be utilized as follows. By using the vacuum pump and the argon tank, air can be essentially removed from the flow line, and a vacuum as low as 5×10^{-3} torr can be achieved. The solution vessel can be detached from the system for solution preparation and degassing, and then reattached for the kinetic run. The flow line can be filled with argon gas, and then an over-pressure of argon gas can push the solution into the sample cell for a flash and on into the waste vessel after that run. The waste vessel can be detached from the system for solvent recovery. With a bulk amount of solution made in the solution vessel (around 200 ml), many runs can be performed before having to prepare a new solution of reactants.

The Data Acquisition and Analysis System

The indium antinomide detector is wired through an amplifier into a LeCroy Model 9410 digital oscilloscope, which captures the absorbance vs. time data for each run in binary format. The "absorbance" values read by the oscilloscope, of course, are really voltage values, and mathematical manipulation is required to produce the actual absorbance vs. time data. This digital oscilloscope is hooked into an IBM-comaptible personal computer through a GPIB board.

It was a challenge to find the best method to perform the kinetic analyses on the raw data captured by the oscilloscope. The original intent was to utilize four programs

borrowed from Northwestern University that could capture the waveforms from the oscilloscope, display and manipulate these waveforms, and perform exponential and double exponential curve fits on the data. However, these programs were not compatible with the system described here for a number of reasons, the most important being differences in oscilloscopes. With modifications, the Northwestern programs could have been made to work, but no one in the research group had the Fortran programming ability to make these changes.

Thus, a search was carried out to find alternative methods to perform the kinetic analyses. A method was finally settled upon which is related below. The LeCroy Corporation provided free software designed to control the Model 9410 oscilloscope and download waveforms. The program 94G can download the captured decay curves in binary format, and the program 94TRAN could then be used to convert the binary files into ASCII format. A Fortran application called VOLTAGES, written by Sue Richter (11), is used to convert the voltage values to absorbance values and then saves a data file which can be used by Axum, a technical graphics software package available commercially. Two macros were written by myself within Axum which read in the data files from VOLTAGES and calculate ln A and 1/A values. Axum can then be used to make the A vs. t, ln A vs. t and 1/A vs. t plots necessary in a kinetic analysis. Linear fits can be made on the kinetic plots to determine reaction order and rate constants (from the slopes of those best fit lines). Single exponential fits to the absorbance vs. time data can also be performed when the reactions are following first order kinetics.

Chapter 3: Dimanganese Decacarbonyl Studied by FTRUV/VIS Spectroscopy (Experimental)

It was important to do a preliminary study on the dimanganese decacarbonyl photochemical system using the UV/VIS flash rig for a number of reasons. The main interest in this experiment involved testing parts of the experimental method used with the new FTRIR flash rig described in the last chapter. In this case, much of the synthetic technique for preparing the dimanganese decacarbonyl solutions and the data analysis set-up are utilized identically with both flash rigs. By performing the experiment with the already built UV/VIS flash rig, these aspects of the FTRIR rig's operation could be perfected. This experiment was also important because it provided a relatively simple method of looking at this photochemical system which lends itself well to use in the Physical Chemistry laboratory at Union College. As seen in Chapter 1, the photochemical reactions of dimanganese decacarbonyl proceeded by both second and pseudo-first order reactions. Because of this property, it provided a system in which a complete picture of reaction kinetics on the first and second order level could be observed by students in the Physical Chemistry laboratory.

In this chapter, various aspects of this experiment will be discussed in detail.

Solvent Purification

The main solvent used for the dissolution of dimanganese decacarbonyl in this experiment was cyclohexane. It has been mentioned before that this transition metal carbonyl is sensitive to both air and water. Thus, it was of extreme importance to remove as much water and dissolved oxygen from the solvent before use. In this case, a reflux apparatus was utilized for purification. A constant flow of argon gas was pushed through the reflux apparatus so that no air would be present in the system during the reflux process. The cyclohexane solvent (Aldrich, 99.9+%) was then refluxed over granular

calcium hydride (CaH_2) for at least 15 hours to ensure removal of water and dissolved oxygen.

Solution Preparation

A solution of approximately 1 x 10^{-4} M dimanganese decacarbonyl in cyclohexane was prepared by the following method. A sufficient quantity of the refluxed cyclohexane (approximately 250 ml) was first collected from the reflux apparatus, again under flowing argon gas. The cyclohexane, dimanganese decacarbonyl crystals and all necessary equipment was put inside a nitrogen-filled glove bag where the solution preparation would take place. About 13 mg of dimanganese decacarbonyl crystals was weighed into a 25 ml volumetric flask, which was then filled with cyclohexane. Then, 2 ml of this solution was transferred into another 25 ml volumetric flask, where it was diluted. This solution was approximately 1 x 10^{-4} M.

The solution was poured into the solution vessel used with the UV/VIS flash rig, pictured in Figure 6, and attached to the high vacuum line nearby. Within the cold finger, six freeze-pump-thaw cycles were performed on the solution with the intent of removing any dissolved oxygen from the solvent that might be remaining. A freeze-pump-thaw cycle consisted of the following. The solution was frozen using a liquid nitrogen bath, and the vessel was opened to vacuum. When the atmosphere above the solution was pumped out, the vessel was closed and the solution was allowed to thaw back to room temperature. Any dissolved gases within the solvent proceeded to bubble out of solution until the pressure differential was remedied. Six of these cycles was enough to essentially degas the reaction solution. The solution was then poured from the cold finger into the quartz optical cell attached to the vessel. This optical cell was placed in the probe beam of the UV/VIS flash rig for use in the experiment.

The freeze-pump-thaw cycles differed somewhat when we wished to induce pseudo-first order kinetics. The solution was frozen using an acetone slush (-96°C) which

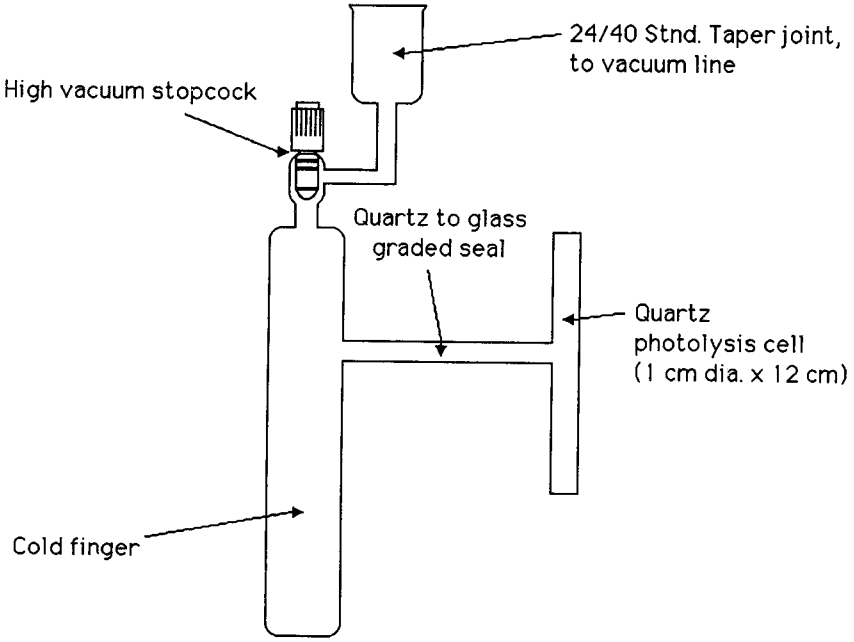

Figure 6: Diagram of sample cell for UV/VIS flash rig

would freeze the solution without freezing out added carbon monoxide gas. This CO(g) (Matheson Research Grade, 99.99% pure) was introduced over the solution, and its pressure was measured with a mercury manometer. The reaction vessel was closed, warmed to room temperature and stirred for 15 minutes. The concentrations of CO that dissolved in the cyclohexane solvent at each pressure could be determined using Henry's Law.

Description of the Flash Rig

A schematic of the UV/VIS flash rig can be found in Figure 7. The rig itself is described in greater detail in a recent publication (12). The photolysis source is the same one used in the FTRIR flash rig described in the previous chapter with two xenon flashlamps positioned on either side of the sample cell. Filter solutions can be used in conjunction with the lamps to filter out wavelengths of light that could interfere with the absorbance measurements. The probe beam is provided by a xenon arc lamp, which outputs a polychromatic beam in the UV/VIS spectrum. A monochromator at the detector end of this beam filters out all wavelengths but the one wavelength of interest. A photomultiplier tube (PMT) serves as the detector for the rig, and absorbance measurements from the PMT are transferred through an electronic amplifier into the LeCroy digital oscilloscope mentioned in Chapter 2. The data analysis train used here, including the IBM compatible computer, is identical to the one utilized on the FTRIR flash rig.

Experimental Procedure

The first step in this experiment was to prepare the reaction solution by the method described above. After the freeze-pump-thaw cycles were completed and the solution was placed in the probe beam (within the optical cell), the solution was flashed with the flashlamps. The absorbance of the reaction intermediates being observed (either

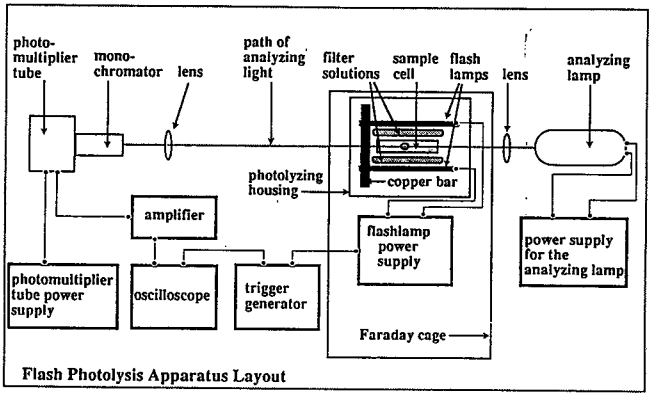

Figure 7: Schematic of the UV/VIS flash rig

$Mn_2(CO)_9$ or $Mn(CO)_5$) was recorded as a function of time using the PMT detector. This decay curve could then be transferred to the computer using the method discussed in Chapter 2, and finally Axum could be used to perform the kinetic analysis and to generate plots.

Chapter 4: Dimanganese Decacarbonyl Studied by FTRUV/VIS Spectroscopy (Results)

$Mn_2(CO)_{10}$ Photochemistry

For this system, there are two separate UV/VIS absorption peaks, each due to one of the reaction intermediates. Dimanganese nonacarbonyl absorbs at 500 nm, while manganese pentacarbonyl absorbs at 827 nm. A typical absorbance vs. time plot for each of these intermediates can be seen in Figures 8 and 9. An observation can be made here regarding reaction time scales. As expected, the $Mn_2(CO)_9$ ligand recombination reaction (Figure 8) proceeds at a much slower rate than the $Mn(CO)_5$ "fast" radical recombination reaction (Figure 9). But in both cases a large absorbance peak can be observed initially, where the flash activates the dimanganese decacarbonyl. This peak is followed by a slower decay back to the baseline, where the intermediates recombine to form the parent compound.

The computational capabilities of the Axum software could be used to produce plots of ln A vs. time and 1/A vs. time, which are seen in Figures 10-13. Referring to the kinetics discussion in Chapter 1, it is known that if the plot of ln A vs. time is linear, the reaction is first order. Likewise, if the plot of 1/A vs. time is linear, the reaction is second order. It can be seen from the figures that both reactions are second order, as would be expected for simple recombination reactions. The line in Figure 11 should correspond to Equation 13 in Chapter 1, while the line in Figure 13 should correspond to Equation 14. Thus, the slopes from these lines could be used to calculate the rate constants of these two recombination reactions.

$$\text{Slope from Figure 11} = k_1/(\varepsilon \bullet l) \qquad (19)$$

$$\text{Slope from Figure 13} = (2\,k_2)/(\varepsilon \bullet l) \qquad (20)$$

However, a problem arises at this point in the calculation, since the path length l is known but the extinction coefficients ε for $Mn_2(CO)_9$ and $Mn(CO)_5$ are not known. Values for k/ε can be determined, however.

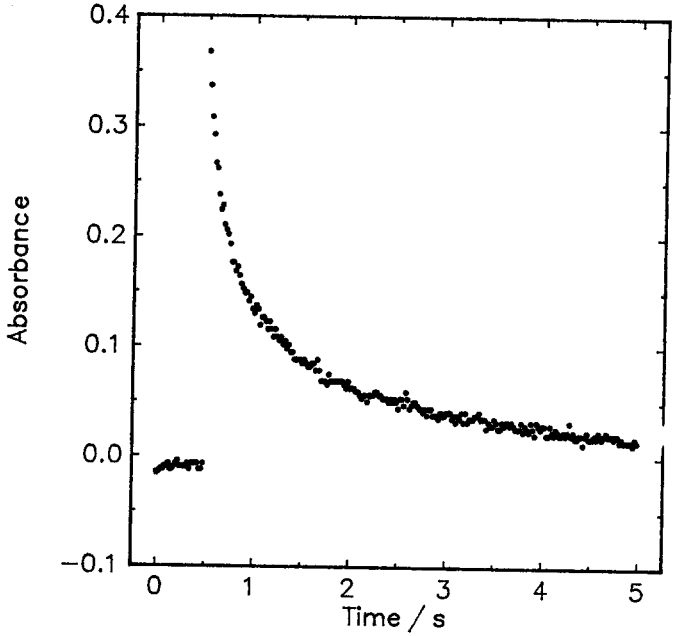

Figure 8: Absorbance vs. time plot for $Mn_2(CO)_9$ monitored at 500 nm

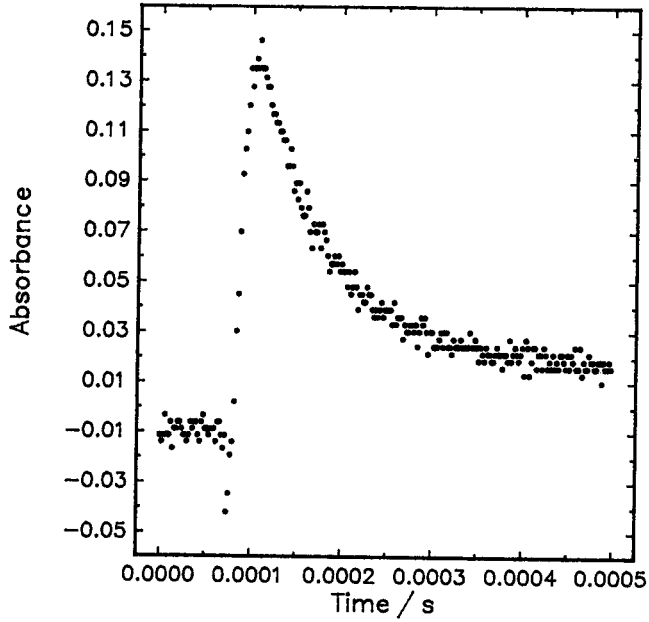

Figure 9: Absorbance vs. time plot for $Mn(CO)_5$ monitored at 827 nm

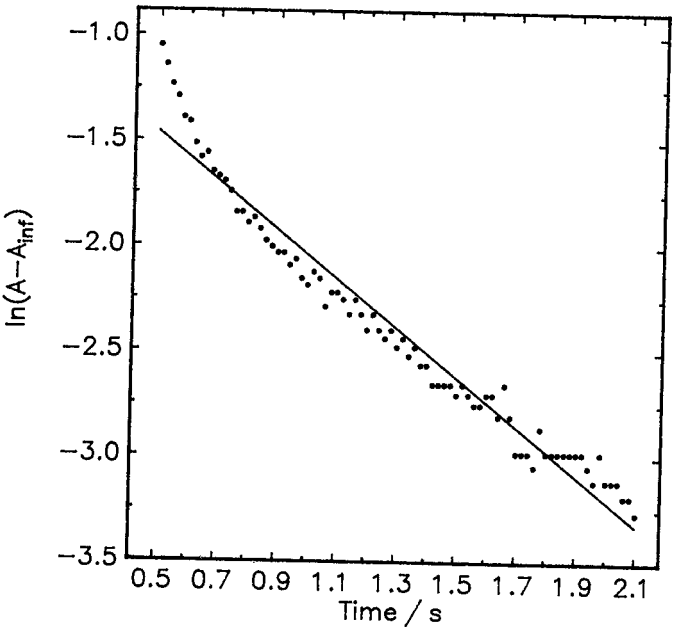

Figure 10: ln (A-A_{inf}) vs. time plot for $Mn_2(CO)_9$ monitored at 500 nm

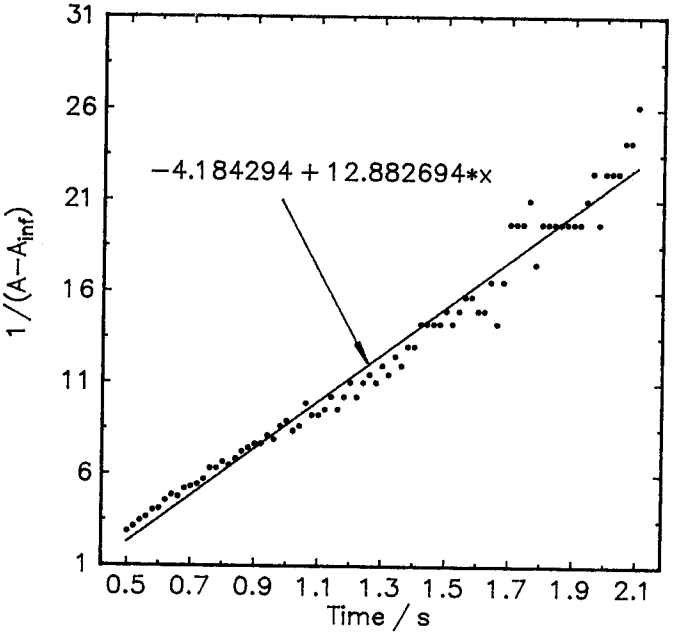

Figure 11: $1/(A-A_{inf})$ vs. time plot for $Mn_2(CO)_9$ monitored at 500 nm

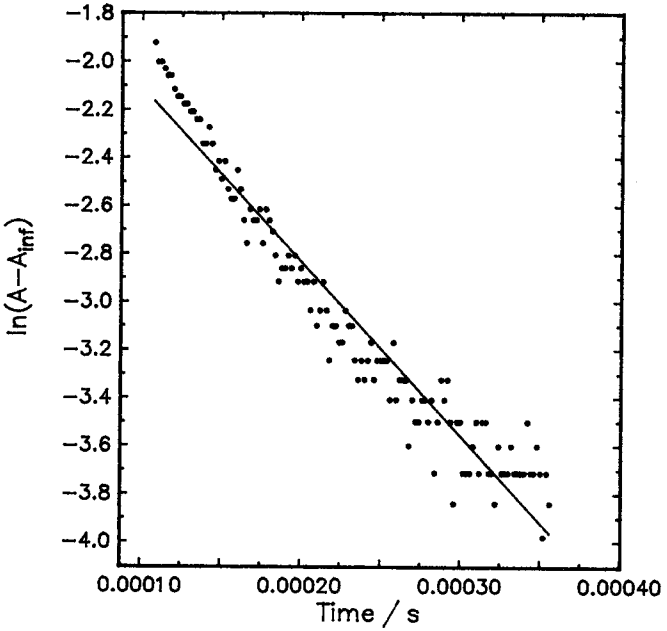

Figure 12: ln (A-A_{inf}) vs. time plot for $Mn(CO)_5$ monitored at 827 nm

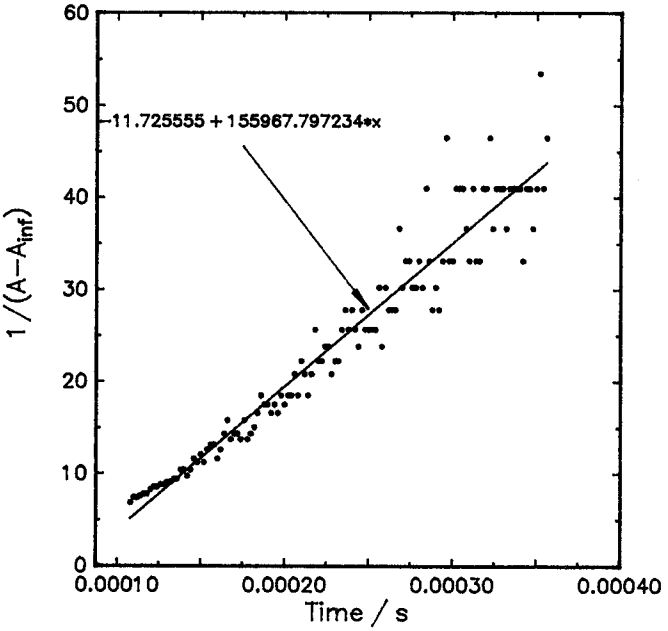

Figure 13: $1/(A-A_{inf})$ vs. time plot for $Mn(CO)_5$ monitored at 827 nm

$$k_1/\varepsilon_{500} = \text{Slope} \bullet l = (13\ s^{-1})(12\ cm) = 156\ cm\ s^{-1} \quad (21)$$

$$k_2/\varepsilon_{827} = (\text{Slope} \bullet l)/2 = [(1.6 \times 10^5\ s^{-1})(12\ cm)]/2 = 9.6 \times 10^5\ cm\ s^{-1} \quad (22)$$

For the recombination of the $Mn(CO)_5$ fragments, a value for ε_{827} was reported as 800 $cm^{-1}\ \underline{M}^{-1}$ in the literature (13). Knowing this, the value for k_2 could be calculated.

$$k_2 = (k_2/\varepsilon_{827})\varepsilon_{827} = (9.6 \times 10^5\ cm\ s^{-1})(800\ cm^{-1}\ \underline{M}^{-1}) = 7.7 \times 10^8\ \underline{M}^{-1}\ s^{-1} \quad (23)$$

Both the k_2/ε_{827} and k_2 values show good agreement with the values reported in the literature (Table 1).

$\underline{Mn_2(CO)_{10}}$ Photochemistry with Added CO(g)

It was discussed in Chapter 1 that two techniques could be used if the exact value of ε was not known for the substance being studied. The first was to assume a value for ε based on known extinction coefficient values of similar compounds and other experimental evidence. Yesaka's group determined an upper limit for the ε_{500} value of 1000 $cm^{-1}\ \underline{M}^{-1}$, and assumed ε_{500} was in its upper limit so that the value of k_1 could be calculated (2). They based their assumption on the known molar absorptivity of $Mn_2(CO)_9(MeCN)$ (1100 $cm^{-1}\ \underline{M}^{-1}$) and the transient absorption spectrum of $Mn_2(CO)_9$ in cyclohexane. The other method was to induce pseudo-first order behavior in the reaction (if possible). This second method was used in the study presented here.

A set of kinetic plots for a run where the dimanganese decacarbonyl solution was placed under an atmosphere of 200 torr CO(g) can be seen in Figures 14-16. It can be seen that now the ln A vs. time plot (Figure 15) was linear, showing that pseudo-first order behavior was induced. This plot corresponds to Equation 15 in Chapter 1, where the slope of the best fit line should equal $-k_{obs}$. Pseudo-first order behavior was induced using a variety of CO(g) overpressures, these being 100, 200, 300, 400 and 500 torr. In each case, a different k_{obs} value was determined. It is known that each of the k_{obs} values is related to the actual rate constant k_1 by this equation.

$$k_{obs} = k_1 \bullet [CO] \quad (24)$$

Table 1: Compiled Values for the Rate Constant of the Reaction $2\ Mn(CO)_5 \rightarrow Mn_2(CO)_{10}$

Reference	(k_2/ε_{827}) / cm s^{-1}	k_2 / M^{-1} s^{-1}
Church, et al.	8.8×10^5	7×10^8 [a]
Our findings	9.6×10^5	7.7×10^8 [a]
Yesaka, et al.	$11. \times 10^5$	8.8×10^8 [a]
Hughey, et al.	--	$39. \times 10^8$ [b]

Yesaka, et al. *JACS*, 1983, 105, 6249-52.
Hughey, et al. *J. Organomet. Chem.*, 1977, 125, C49-C52.
Church, et al. *J. Chem. Soc., Chem. Commun.*, 1984, 785-6.

[a]This value was found assuming an ε_{827} value of 800 cm^{-1} M^{-1} (found in Waltz et al. *JACS*, 1978, 100, 7259.).

[b]This value was found by monitoring directly the production of $Mn_2(CO)_{10}$, and thus does not assume a value for ε_{827} but rather was measured directly.

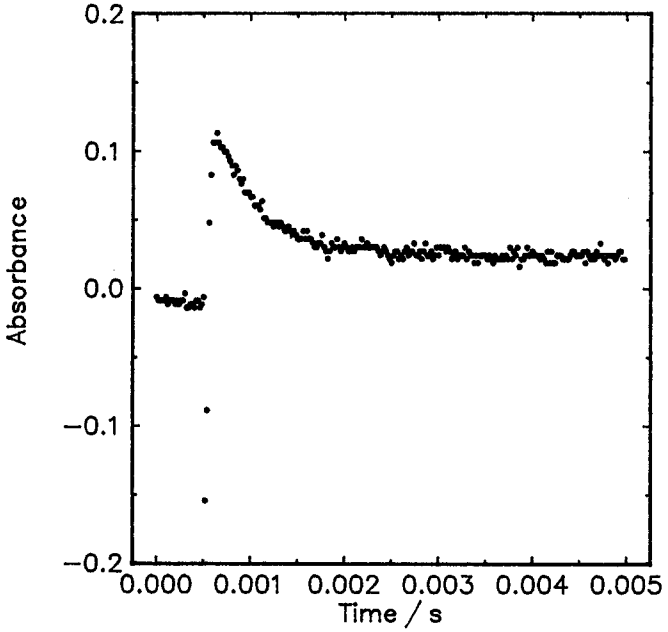

Figure 14: Absorbance vs. time plot for $Mn_2(CO)_9$ under 200 torr CO(g) and monitored at 500 nm

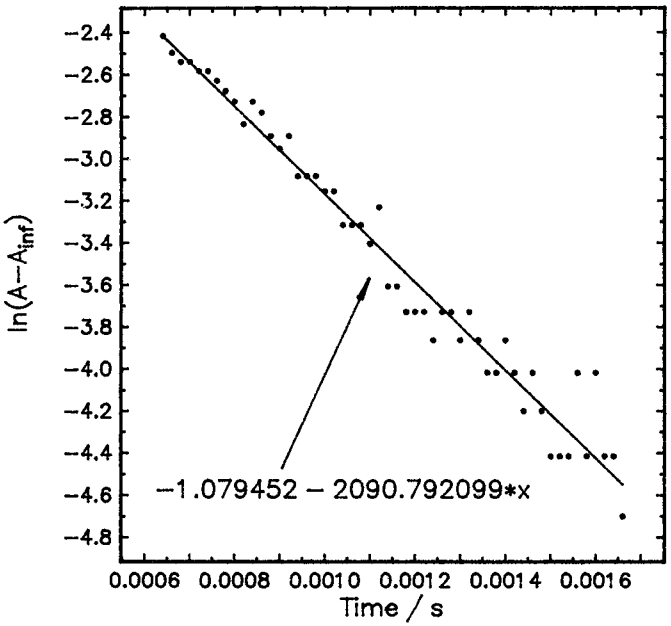

Figure 15: ln (A-A_{inf}) vs. time plot for $Mn_2(CO)_9$ under 200 torr CO(g) and monitored at 500 nm

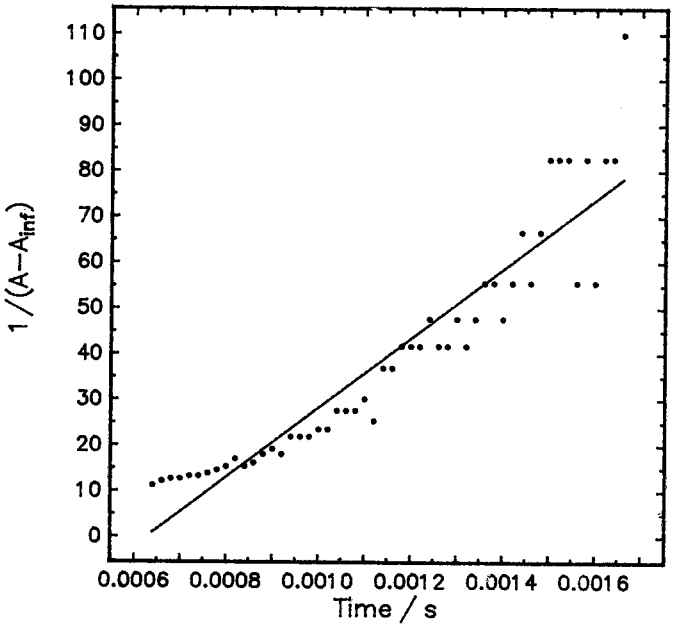

Figure 16: $1/(A-A_{inf})$ vs. time plot for $Mn_2(CO)_9$ under 200 torr CO(g) and monitored at 500 nm

It is obvious, then, that a plot of the k_{obs} values as a function of the molar concentration of dissolved CO (found using Henry's Law) should be linear, and the slope should equal the second order rate constant for the $Mn_2(CO)_9$ recombination reaction, k_1. From Figure 17, it is found that $k_1 = 6.9 \times 10^5\ \underline{M}^{-1}\ s^{-1}$. This value for k_1 falls within expected values, as reported in various publications (Table 2).

By calculating the value for k_1 without assuming a value for ε_{500}, an experimentally determined value for ε_{500} can subsequently be found.

$$\varepsilon_{500} = k_1/(k_1/\varepsilon_{500}) = (6.9 \times 10^5\ \underline{M}^{-1}\ s^{-1})/(156\ cm\ s^{-1}) = 4.4 \times 10^3\ cm^{-1}\ \underline{M}^{-1} \quad (25)$$

It can be seen that the experimentally determined extinction coefficient does not agree well with Yesaka's assumed value of 1000 $cm^{-1}\ \underline{M}^{-1}$. Since the value reported here was determined experimentally from the absorbing species rather than assumed from a chemically similar compound (in this case, $Mn_2(CO)_9(MeCN)$), one would have to give more credibility to our experimentally determined value.

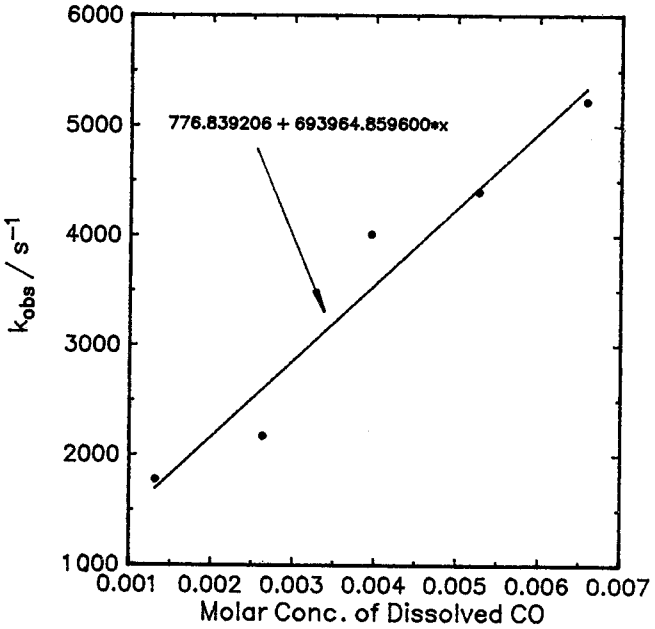

Figure 17: k_{obs} vs. [CO] plot for $Mn_2(CO)_9$

Table 2: Compiled Values for the Rate Constant of the Reaction $Mn_2(CO)_9 + CO \rightarrow Mn_2(CO)_{10}$

Reference		(k_1/ε_{500}) / cm s^{-1}	k_1 / M^{-1} s^{-1}
Yesaka, et al.		120	1.2×10^5 [a]
Herrick, et al.		--	2.9×10^5 [b]
Our findings		156	6.9×10^5
Church, et al.	UV/VIS det.	500	7.5×10^5
	IR detection	--	$12. \times 10^5$

Yesaka, et al. *JACS*, 1983, 105, 6249-52.
Hughey, et al. *J. Organomet. Chem.*, .977, 125, C49-C52.
Church, et al. *J. Chem. Soc., Chem. Commun.*, 1984, 785-6.

[a]This value was found assuming an ε_{500} value of 1000 cm^{-1} M^{-1}.

[b]This value is for the $Mn_2(CO)_{10}$ system, but the solvent used was hexane rather than cyclohexane.

Chapter 5: Dimanganese Decacarbonyl Studied by FTRIR Spectroscopy

After completing the construction of the FTRIR flash rig, a project was started with the intent to observe the kinetics of dimanganese decacarbonyl photochemistry. The results from this study could be compared with the results of the UV/VIS absorption spectroscopy study described in Chapters 3 and 4, and also with reported literature values. These comparisons should give an idea of the accuracy of results taken with this new piece of laboratory apparatus. However, science isn't always perfect and theory sometimes does not translate into reality. Therefore, this study of dimanganese decacarbonyl afforded an opportunity to perform some troubleshooting on the FTRIR flash rig. Although no kinetic data has yet been collected using the new instrument (at the time of this writing), the preliminary work has highlighted some problems which we have had to address. These are described below.

Solution Preparation and Properties

The first aspect of the study was to formulate a method of preparing the dimanganese decacarbonyl solutions. Since the solution was to be used in a flow system (pictured in Figure 5), it was necessary to create these solutions in bulk (on the order of 200 ml). Another change involved the choice of solvent. It was important to pick the most IR-transparent solvent for use in this system, and thus heptane replaced cyclohexane as the solvent of choice for this system. In a nitrogen-filled glove bag, approximately 9 mg of $Mn_2(CO)_{10}$ crystals were weighed into a tared 200 ml volumetric flask, which was then filled with heptane. This solution (approximately 1×10^{-4} M) was poured into the solution vessel used with the flow system. Freeze-pump-thaw cycles could be performed to degas this solution before use.

A FTIR spectrum of the solution prepared above is provided in Figure 18. This spectrum was prepared by a subtraction method where the spectrum of pure heptane was subtracted from the spectrum of dimanganese decacarbonyl dissolved in heptane, thus

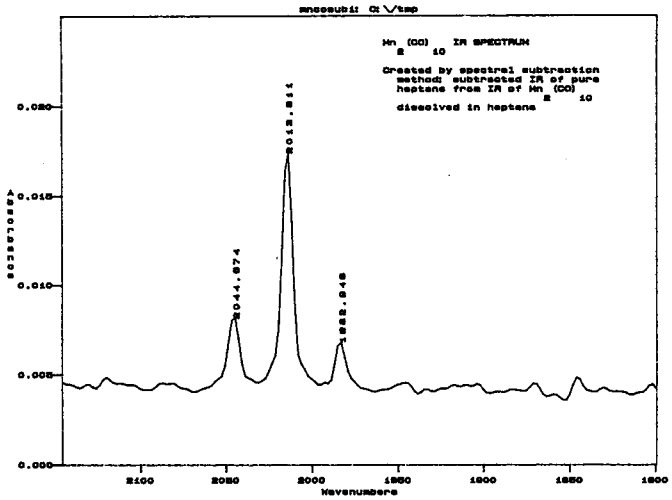

Figure 18: FTIR spectrum of $Mn_2(CO)_{10}$

creating a spectrum of dimanganese decacarbonyl itself. Three peaks of note can be seen in the spectrum itself, which are IR absorbances of the parent compound. From the series of IR absorbance peaks of the two intermediates listed in Church's publication (3), monitoring peaks for $Mn_2(CO)_9$ and $Mn(CO)_5$ had to be chosen which did not overlap with those of the parent compound. For the work here, we chose to observe $Mn_2(CO)_9$ at 1968 cm^{-1}, and $Mn(CO)_5$ at 1988 cm^{-1}.

Debugging the Instrument

Various problems were encountered during the process of analyzing the kinetics of dimanganese decacarbonyl photochemistry. Of these, two were most prominent. The first involved the path length of the sample cell. The rubber O-rings being used to seal the sample cell were much too thick. The path length with the original O-rings was estimated to be around 4-5 mm, which is much larger than typical path lengths used in IR spectroscopy of solutions. The beam from the diode laser was lost when passed through the filled sample cell because of the IR absorbing properties of the solvent, and thus the path length needed to be reduced. This reduction was tempered by another problem, that of air-tightness. The first replacement O-rings were fashioned from Buna-N cord (with a rubber glue) and were of approximately 0.5 mm thickness. Unfortunately, it was discovered that these O-rings could not hold a vacuum seal of less than 20 torr, which indicated substantial leakage of air around the O-rings. A gasket design was tried next rather than an O-ring design, which provided a minimal thickness (again, around 0.5 mm) with more surface area contacting with the CaF_2 plates, thus improving the air-tightness of the cell. Buna-N rubber was used for the first set of gaskets, but it was discovered that Buna-N dissolved rather readily in heptane (over a 24 hour period). If the reactions were left in the sample cell for hours, they would be contaminated by this dissolution process. Finally, Viton gaskets of the same thickness were used, which proved to be more resistant to degradation by the heptane solvent. These gaskets could hold a vacuum of about 0.005

torr, which is the limit of our vacuum pump, and allowed a significant amount of the IR probe beam through the solution. With the implementation of these gaskets, the path length of the optical cell was reduced to approximately 1.25 mm.

The second problem stemmed from electronic transients present within the system. This problem was solved to a large extent with the use of Faraday cages. Initially, the micropulser and the flash housing were enclosed in two copper mesh Faraday cages. With this set-up, though, an appreciable amount of electronic artifacts could still be seen with the oscilloscope. It was thought that these artifacts were being transmitted by the unshielded wires connecting the electronics of the system. These cables were shielded with a flexible copper mesh tubing which acts as a Faraday "tunnel" and eliminates through-space electronic transients. This improved the situation, but there were still some disturbing transients being observed. A new Faraday cage was very recently built using copper sheeting to house the remaining unshielded electronics, including the detector and the amplifier.

Current Standing

At present, much of the electronic artifacts have been eliminated by the shielding described above. With the addition of the detector Faraday cage, the transients were reduced to a very short-lived peak appearing near the time of the flash. This transient is pictured in Figure 19, which is an absorbance vs. time decay curve captured using the FTRIR flash rig on pure heptane. This spectrum should appear as a flat line, but a definite transient absorbance peak is seen to appear and then rapidly disappear. It is thought that by improving the existing Faraday cages (i.e. replacing the copper mesh with copper sheeting), this final transient could be further reduced if not eliminated.

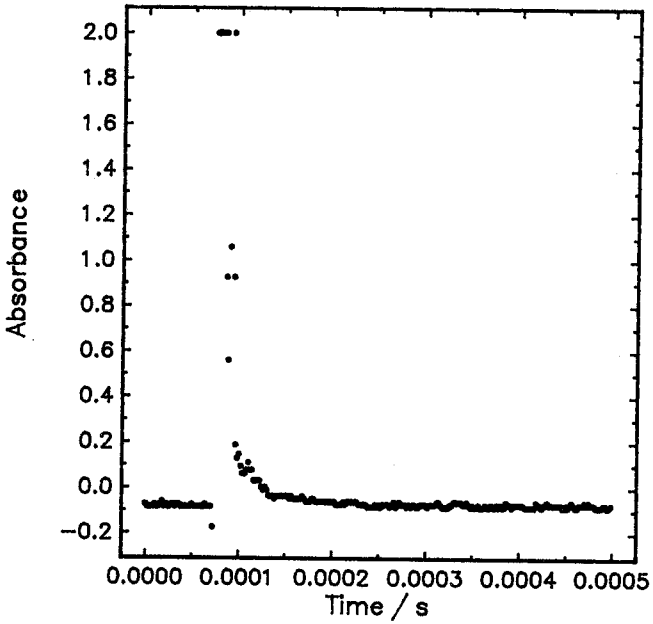

Figure 19: Absorbance vs. time plot for heptane taken on the FTRIR flash rig

Chapter 6: Beyond Dimanganese Decacarbonyl

In conclusion, the future direction of this project will be outlined here. Dimanganese decacarbonyl does provide a good test system for the FTRIR flash rig, with its simple photochemistry. But performing the kinetic study of this transition metal carbonyl, even with the use of FTRIR absorption spectroscopy, is not particularly ground-breaking reserach, as there have been numerous studies already performed on the compound (1-9). So, the first step into the future would be to complete the kinetic study of dimanganese decacarbonyl in order to test the performance of the new instrument.

With the successful completion of the $Mn_2(CO)_{10}$ kinetic study, it is hoped that another "spin-off" experiment can be developed for the Physical Chemistry laboratory. This new experiment would allow chemistry students at Union College to receive exposure to cutting-edge experimental techniques during their undergraduate chemistry experience.

When the performance of the FTRIR flash rig is validated, the research group can proceed to new photocatalytic systems which use transition metal carbonyls as photocatalysts. The first system of this type is the hydrosilation of ethylene catalyzed by $Et_3SiCo(CO)_4$. A mechanism for this catalytic cycle was proposed by Wrighton and Seitz in 1988 (14), and is shown in Figure 20. The reaction intermediates shown there have never been directly observed by any means, but were proposed with indirect experimental evidence. With the new FTRIR flash rig, it is hoped that several of these intermediates can be directly observed through absorption spectroscopy, especially the primary photolysis product (product of reaction #1) and the ethylene-substituted complex (product of reaction #2). Kinetic data can also be collected for the various steps in the cycle, giving more insight into the workings of this complex catalytic cycle.

The new apparatus should allow the research group to study the kinetics and mechanisms of a variety of transition metal carbonyl catalyzed organic reactions, which

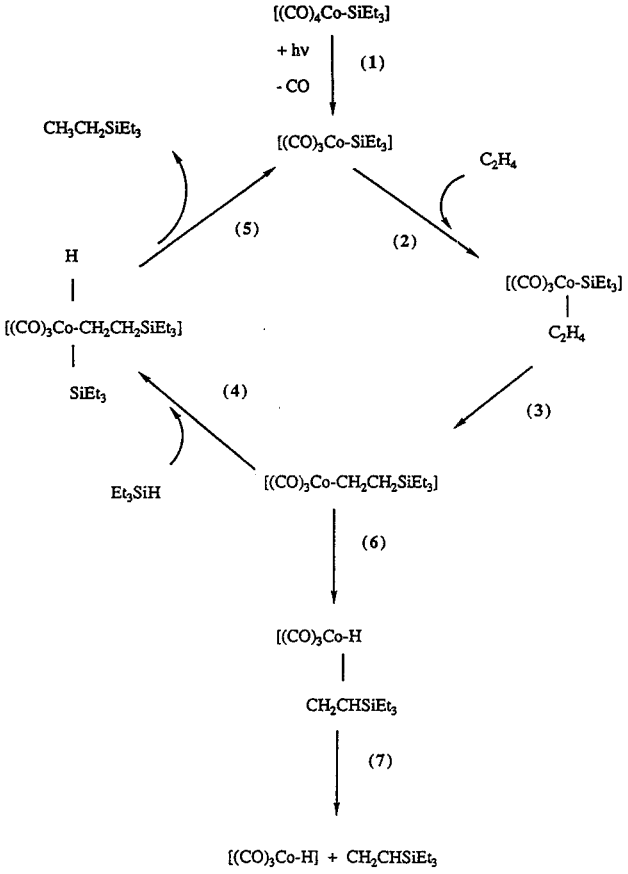

Figure 20: Catalytic cycle for the hydrosilation of ethylene catalyzed by $Et_3SiCo(CO)_4$

will provide many opportunities for doing organometallic chemistry research at Union College.

References

(1) Hughey, J.L., IV; Anderson, C.P.; Meyer, T.J. *Journal of Organometallic Chemistry* **1977**, *125*, C49-C52.

(2) Yesaka, H.; Kobayashi, T.; Yasufuku, K.; Nagakura, S. *J. Am. Chem. Soc.* **1983**, *105*, 6249-6252.

(3) Church, S.P.; Hermann, H.; Grevels, F.W.; Schaffner, K. *J. Chem. Soc., Chem. Commun.* **1984**, 785-786.

(4) Kidd, D.R.; Brown, T.L. *J. Am. Chem. Soc.* **1978**, *100*, 4095-4102.

(5) Wegman, R.W.; Olsen, R.J.; Gard, D.R.; Faulkner, L.R.; Brown, T.L. *J. Am. Chem. Soc.* **1981**, *103*, 6089-6092.

(6) Church, S.P.; Poliakoff, M.; Timney, J.A.; Turner, J.J. *Inorg. Chem.* **1983**, *22*, 3259-3266.

(7) Hepp, A.F.; Wrighton, M.S. *J. Am. Chem. Soc.* **1983**, *105*, 5934-5935.

(8) Herrick, R.S.; Brown, T.L. *Inorg. Chem.* **1984**, *23*, 4550-4553.

(9) Seder, T.A.; Church, S.P.; Weitz, E. *J. Am. Chem. Soc.* **1986**, *108*, 7518-7524.

(10) Bernard, E.J.; "The Construction of an Apparatus to Do Fast Transient IR Spectroscopy"; Thesis Union College, **1991**.

(11) Richter, S.R.; "Construction of an Instrument for Doing Fast Time-Resolved Infrared Spectroscopy"; Thesis Union College, **1992**.

(12) Clark, L.M.; Hayes, S.E.; Hayes, D.M.; McFarland, J.M.; Miller, R.L.; Shalmi, C.L.; Soltis, M.G.; Susnow, R.; Strong, R.L. *J. Chem. Ed.* **1992**, *69*, 336-339.

(13) Waltz, W.L.; Hackelberg, O.; Dorfman, L.M.; Wojcicki, A. *J. Am. Chem. Soc.* **1978**, *100*, 7259.

(14) Seitz, F.; Wrighton, M.S. *Angew. Chem. Int. Ed. Engl.* **1988**, *27*, 289-291.